
**Acquisition of epibiotic bacteria along the life cycle of the hydrothermal shrimp
*Rimicaris exoculata***Mathieu Guri^{1,*}, Lucile Durand², Valérie Cueff-Gauchard², Magali Zbinden³, Philippe Crassous²,
Bruce Shillito³ and Marie-Anne Cambon-Bonavita²¹ CNRS, LM2E, UMR6197, BP70, Plouzané, France² Ifremer, DEEP/Laboratoire de Microbiologie des Environnements Extrêmes, UMR6197, Technopôle Brest Iroise, BP70, Plouzané, France³ UMR CNRS 7138, Systématique, Adaptations et Evolution, Université Pierre et Marie Curie, Paris, France*: Corresponding author : Mathieu Guri, email address : Mathieu.guri@gmail.com

Abstract:

The caridean shrimp *Rimicaris exoculata* dominates the fauna at several Mid-Atlantic Ridge hydrothermal vent sites. This shrimp has an enlarged gill chamber, harboring a dense ectosymbiotic community of chemoautotrophic bacteria associated with mineral oxide deposits. Until now, their acquisition is not fully understood. At three hydrothermal vent sites, we analyzed the epibionts diversity at different moult stages and also in the first stages of the shrimp life (eggs, hatched eggs (with larvae) and juveniles). Hatched eggs associated with young larvae were collected for the first time directly from gravid females at the Logachev vent site during the Serpentine cruise. An approach using 16S rRNA clone libraries, scanning and transmission electron microscopy, and fluorescent *in situ* hybridization was used. Molecular results and microscope observations indicated a switch in the composition of the bacterial community between early *R. exoculata* life cycle stage (egg libraries dominated by the *Gammaproteobacteria*) and later stages (juvenile/adult libraries dominated by the *Epsilonproteobacteria*). We hypothesized that the epibiotic phylotype composition could vary according to the life stage of the shrimp. Our results confirmed the occurrence of a symbiosis with *Gammaproteobacteria* and *Epsilonproteobacteria*, but more complex than previously assumed. We revealed the presence of active type-I methanotrophic bacteria colonizing the cephalothorax of shrimps from the Rainbow site. They were also present on the eggs from the Logachev site. This could be the first 'epibiotic' association between methanotrophic bacteria and hydrothermal vent crustacean. We discuss possible transmission pathways for epibionts linked to the shrimp life cycle.

Keywords: symbiosis; larvae; methanotrophic symbiont; *Rimicaris exoculata*; transmission pathways

86 Introduction

87 Trophic symbioses are common in deep-sea hydrothermal ecosystems. In
88 these environments, symbiosis between chemosynthetic bacteria and
89 invertebrates supports a strikingly diversified fauna and significantly more
90 biomass than in surrounding seawater (Ruehland *et al.*, 2010, Goffredi *et al.*,
91 2010; Bates *et al.*, 2011). One of these invertebrates is the shrimp *Rimicaris*
92 *exoculata* (Williams and Rona, 1986). This crustacean, belonging to the family
93 *Alvinocarididae*, is part of the dominant megafauna at several Mid-Atlantic
94 Ridge (MAR) vent sites (Desbruyères *et al.*, 2001), where it forms dense and
95 motile aggregates around the chimney walls (Segonzac, 1992; Gebruk *et al.*,
96 1993). *R. exoculata* harbours a rich community of epibiotic bacteria on the inner
97 side of its enlarged gill chamber (also called cephalothorax) and on its
98 mouthparts (scaphognathites and exopodites of the first maxillipeds, both
99 covered with abundant bacteriophage setae). These characteristics were
100 encountered in all *R. exoculata* specimens regardless of the site (Van Dover *et*
101 *al.*, 1988; Casanova *et al.*, 1993; Segonzac *et al.*, 1993; Zbinden *et al.*, 2004),
102 highlighted a possible obligate relationship between the shrimp and its epibionts.
103 A $\delta^{13}\text{C}$ stable isotope study showed that the predominant source of dietary
104 carbon for the shrimp was the gill chamber epibionts (Rieley *et al.*, 1999), but
105 the bacterial community in the shrimp gut has also been proposed as an

106 alternative nutritional source (Polz *et al.*, 1998; Pond *et al.*, 2000; Zbinden *et al.*,
107 2003; Durand *et al.*, 2010).

108 Recent studies have shown that the diversity of *R. exoculata* epibionts was
109 higher than previously reported (Zbinden *et al.*, 2004, 2008; Petersen *et al.*,
110 2009; Hügler *et al.*, 2011). Based on *in vivo* experiments (IPOCAMPTM (Shillito
111 *et al.*, 2004)), microscopic and molecular analyses, the co-occurrence of three
112 metabolisms (iron, sulfur, and methane oxidation) among gill chamber epibiont
113 communities has been proposed (Zbinden *et al.*, 2008). Moreover the *pmoA* and
114 *aps* genes were amplified. It was also suggested that the relative contribution of
115 each metabolism might differ according to fluid chemical composition (Zbinden
116 *et al.*, 2008; Schmidt *et al.*, 2008). Two filamentous epibiont phylotypes
117 (*Gamma* and *Epsilonproteobacteria*) dominated the *R. exoculata* epibiosis and
118 the sequences clustered spatially across the different vent sites along the MAR
119 (Petersen *et al.*, 2009). Finally, the occurrence of autotrophic carbon fixation
120 (rTCA cycle) via sulfur and hydrogen oxidation and sulfur reduction was
121 suggested on the Snake Pit site (Hügler *et al.*, 2011).

122 Like all arthropods, *R. exoculata* undergoes moults, which regularly
123 eliminate the bacterial community settled on the cuticle. The moult cycle
124 seemed to be shortened (10 days) compared to coastal shrimps (*Penaeus*
125 *japonicas* (21 days), *Macrobrachium rosenbergii* (41 to 98 days)) (Corbari *et*
126 *al.*, 2008). Briefly, the shrimps are white after moulting, turn to grey or light red

127 in the mid phase and black or red in the late phase according to the sulfur or iron
128 fluid concentration respectively (Corbari *et al.*, 2008). Microscopic observations
129 showed that a new epibiotic community started to form on free-surfaces of the
130 new cuticle within 2 days after exuviations (Corbari *et al.*, 2008).

131 *R. exoculata* life cycle is still unknown. It produces lipid-rich orange eggs
132 (Llodra *et al.*, 2000), which suggested the occurrence of planktotrophic larvae.
133 Usually, egg size is about 300 to 400 μm (up to 836 eggs/female) (Tyler and
134 Young, 1999). Gametogenic synchrony has never been observed (Tyler and
135 Young, 1999), but a polymodal population structure for this shrimp suggested
136 periodic recruitment (Copley *et al.*, 1998). Up to now, only very few gravid
137 females have been collected and no larvae have ever been collected around the
138 vent sites. Only juveniles above 1.2 cm were collected at the aggregates
139 periphery and are orange (Komai and Segonzac, 2008). Wax esters, fatty acids,
140 and fatty alcohols found in the juveniles indicated that they might feed for
141 extended periods in the euphotic zone, allowing dispersion (Pond *et al.*, 1997).
142 This was supported by genetic data that suggested high gene flow in *R.*
143 *exoculata* populations (Teixeira *et al.*, 2011).

144 In this study, we analyzed the diversity and development of epibionts in
145 *R. exoculata* gill chamber at different moult stages and also in the first stages of
146 shrimp life (eggs, hatched eggs and 2 cm juveniles). An approach using 16S
147 rRNA clone libraries, transmission and scanning electron microscopy

148 (TEM/SEM) and fluorescent *in situ* hybridization (FISH) was performed. Our
149 aims were to examine when the first acquisition of epibionts occurs and to
150 determine whether the epibiont community differs between early life stages and
151 adults, and also between moult stages.

152 Materials and Methods

153 **Collection / Selection / Pretreatment.** Specimens of *R. exoculata* were
154 collected at several hydrothermal vents sites along the MAR: at Logachev
155 (14°45'N; 44°57'W; 3037 meters depth) and Ashadze (12°58'N; 44°51'W; 4088
156 meters depth) during the Serpentine cruise (March 2007); at Rainbow (36°13'N;
157 33°54'W; 2350 meters depth) during the MoMARDREAM-Naut cruise (June
158 2007). Shrimps were collected using the suction sampler of the ROV „Victor
159 6000“ or the Nautilie operated from the R/V „*Pourquoi pas ?*“. Once on board,
160 living individuals were dissected into body parts (branchiostegites (LB),
161 scaphognathites (Sc), exopodites, gills, stomach and digestive tract). For
162 molecular studies, animal tissues and eggs, hatched eggs (still associated with
163 young larvae) and orange juveniles (2 cm) were directly frozen (-80°C) and
164 DNA extractions were performed in the laboratory. For transmission and
165 scanning electron microscopy, samples were fixed as previously described
166 (Zbinden *et al.*, 2008), as well as for fluorescence *in situ* hybridization (FISH)
167 (Durand *et al.*, 2010). Shrimps were sorted according to moulting stages
168 (corresponding to a colour gradient: white (first stage), light red or grey (middle

169 stage), red or black (last stage)). Only black shrimps were collected at the
170 Ashadze site. Eggs and hatched eggs were only found at the Logachev site.
171 Seawater near shrimp aggregates (pH 7.3 and T°C=13°C) was also sampled at
172 the Rainbow site.

173 **DNA extraction and PCR amplification.** DNA from Rainbow seawater, adult
174 LB / Sc, eggs, hatched eggs and juveniles (Sc) was extracted using the Fast
175 DNA Pro Soil-Direct Kit (Qbiogen, Santa Ana, CA) (Table S2). Extracted DNA
176 was then purified with Quick-Clean Spin Filters (Qbiogen, Santa Ana, CA).
177 Bacterial 16S rRNA gene fragments were PCR-amplified in 30 cycles at an
178 annealing temperature of 49°C with the general bacterial primer set 8F and
179 1492R (Lane, 1991). They were then purified with a QIAquick PCR purification
180 kit (Qiagen, France).

181 **Cloning and sequencing.** The pooled amplified and purified PCR products
182 were cloned using the TOPO XL Cloning kit (Invitrogen, Carlsbad, CA)
183 following the manufacturer's instructions. The plasmid inserts were controlled
184 by amplification with M13F and M13R primers. Positive clones were then
185 cultured and treated for sequencing at the Biogenouest Platform (Roscoff,
186 France, <http://www.sb-roscoff.fr/SG/>) on an ABI prism 3130 *xl* (Applied
187 Biosystems, Foster City, CA), using the Big-Dye Terminator V3.1 (Applied
188 Biosystems, Foster City, CA).

189 **Phylogenetic analyses.** Sequences (16S rDNA) were compared to those
190 available in databanks using the BLAST online service (Altschul *et al.*, 1990).

191 Unstable (e.g. chimeras) and short sequences were excluded; others were
192 cleaned manually with „EDITSEQ“ (DNA STAR, Madison, WI, U.S.A).
193 Alignment of sequences was performed using the CLUSTALW program
194 (Thompson *et al.*, 1994), further refined manually using the SEAVIEW program
195 (Galtier *et al.*, 1996). All trees were built using PHYLO-WIN (Galtier *et al.*,
196 1996). Phylogenetic analyses were performed on the basis of evolutionary
197 distance (Neighbor-Joining, (Saitou and Nei, 1987)) with Kimura two-
198 parameters correction matrix. The robustness of phylogenetic reconstructions
199 was tested by bootstrap resampling (500) (Felsenstein, 1985). Sequences
200 exhibiting more than 97 % similarity were considered to be sufficiently related
201 and grouped in the same phylotype.

202 The rarefaction curves and Simpson indices were performed using DOTUR (at
203 97% similarity) for all libraries (Schloss and Handelsman, 2005). Simpson index

204 was calculated as: $1 - H_{simpson} = 1 - \left[\frac{\sum_{i=1}^{S_{obs}} S_i(S_i - 1)}{N(N - 1)} \right]$

205 where S_{obs} representing the number of OTUs observed, S_i the number of
206 individuals for one OTUs and N the total number of OTUs. Good's coverage
207 was calculated as a percentage, according to the following relation $C = [1 -$
208 $(n/N)] \times 100$, where n represented the number of phylotypes appearing only once
209 in a library and N being the library size (Good, 1953, Ravenschlag *et al.*, 1999).

210 **Fluorescence *in situ* hybridization (FISH).** The FISH protocol used was
211 described previously (Durand *et al.*, 2010). Whole LB / Sc (adult and juvenile),

212 eggs and hatched eggs (Table S2) were hybridized with several published probes
213 (Table 2). The hybridization temperature was the same for all sample treated
214 (46°C). Observations and imaging were performed using an Apotome Axio
215 Imager Z₂ with a COLIBRI system (Zeiss, Germany).

216 **Scanning electron microscopy (SEM).** LB / Sc, eggs and hatched eggs were
217 dehydrated in ethanol series (30, 50, 70, 95, 100 % ethanol) and for 5h in a
218 critical point dryer CPD 020 (Balzers union, Balzers, Liechtenstein). Finally,
219 samples were gold-coated with an SCD 040 (Balzers Union). Observations and
220 imaging were performed using a Quanta 200 MK microscope (FEI™, Hillsboro,
221 OR) and the *SCANDIUM* acquisition program (Soft Imaging System, Munster,
222 Germany).

223 **Transmission electron microscopy (TEM).** Samples were dehydrated in
224 ethanol and propylene oxide series and then embedded in an epoxy resin
225 (Serlabo). Semi-thin and ultra-thin sections were made using a Reichert-Jung
226 Ultramicrotome (Ultracut R) with a diamond knife. Semi-thin sections were
227 stained with toluidine blue for observations by light microscopy (using an
228 Olympus BX61 microscope). Thin sections were laid on copper grids and
229 stained with uranyl acetate and lead citrate. Observations were carried out on a
230 LEO 912 electron microscope (LEO Electron Optics GmbH, Oberkochen,
231 Germany) equipped with a LaB6 source and operated at 80 kV.

232 **Nucleotide sequence accession numbers.** The sequences from this study are
233 available through GenBank under the following accession numbers: FR797908
234 to FR797966 (16S rRNA sequences).

235 Results

236 **Samples description.**

237 Seawater collected inside Rainbow shrimp aggregates was slightly orange.
238 Shrimps collected at the three sites (Rainbow, Logachev and Ashadze) were
239 sorted at different moult stages, according to their colour, from white (no
240 minerals or bacteria) to dark red or black (mineral oxide deposits). At the
241 ultramafic Rainbow vent field, the end-member was characterized by extremely
242 high concentrations of ferrous iron (Charlou *et al.*, 2002, Douville *et al.*, 2002),
243 explaining the reddish colour of majority of shrimps (Zbinden *et al.*, 2004). At
244 the Logachev vent site, there was a majority of grey/black shrimps,
245 corresponding probably to iron sulfate deposits (Gebruk *et al.*, 1993). For
246 Ashadze, only 6 black specimens were retrieved. Surprisingly, Ashadze fauna
247 was dominated by species usually recovered at the periphery of hydrothermal
248 communities (*Maractis rimicarivora* and *Phyllochaetopterus* sp. nov.) (Fabri *et*
249 *al.*, 2010). All the collected shrimps were alive and active when recovered from
250 the slurp gun bowls, but the Ashadze specimens were less active than the other
251 sites. It should be noted that Ashadze is the deepest hydrothermal site (4080 m)
252 where *R. exoculata* has been identified.

253 Orange juveniles (2 cm stage A larvae (Komai and Segonzac, 2008)) were
254 sampled at the Rainbow and the Logachev sites, in the periphery of adults but
255 close to the aggregates (Fig. S3). For the first time, eggs and hatched eggs were
256 collected at Logachev during the Serpentine cruise in March 2007 from females
257 collected among the shrimp aggregates (Fig. 1a, b). The eggs, orange, were at
258 different maturity stages, from small young eggs (around 200 μm) to mature
259 eggs (around 400 μm), with only one stage per female. The eggs were always
260 hatched beneath the female abdomen so that only free larvae would be released
261 in the environment. The collected larvae were just hatched eggs, probably at a
262 zoeal stage (Fig. 1b). The rostrum was absent. Eyes were present, ovoid, and
263 seemed to be borne on short eyestalks. Orange pigmented spots were observed
264 in the eyes. Four pairs of pereopods were visible, 3 of them were bifid, and bear
265 3 setae at their tip, the 4th was just a bud. Cephalothorax, covered by a loose
266 carapace, contained the same orange lipid droplets observed in eggs. The
267 abdomen was composed of 5 well delimited short segments. A long terminal
268 segment ended with two blades provided with 6 setae. No pleopods were
269 observed.

270 **Microscopic observations.**

271 I). Adult/juvenile gill chamber - SEM observations on cephalothorax
272 pieces (LB: branchiostegite and Sc: scaphognathite) along the moult cycle
273 confirmed the different epibiont morphologies (e.g. rod-shaped, thin and thick
274 long filaments) observed before (Zbinden *et al.*, 2008). Their development

275 seemed to follow a chronological order along the moult cycle: rod-shaped
276 bacterial mat, followed by long filamentous bacteria, as previously described
277 (Corbari *et al.*, 2008). These morphologies were observed at all the sites studied
278 (Rainbow, Logachev, and Ashadze). FISH observations on LB and Sc along the
279 moult cycle, whatever the hydrothermal site, indicated the predominance of
280 *Epsilonproteobacteria* with thick and thin filamentous morphologies (Fig. 2a,
281 b). This was congruent with molecular studies (Table 1) (Polz and Cavanaugh,
282 1995; Zbinden *et al.*, 2008; Petersen *et al.*, 2009; Hügler *et al.*, 2011).
283 *Gammaproteobacteria* signals were also detected to a lesser extent, and were
284 related exclusively to some thin filamentous morphologies (Fig. 2a,b)
285 confirming previous results (Petersen *et al.*, 2009; Hügler *et al.*, 2011). Type I
286 methanotrophic *Gammaproteobacteria* morphologies were observed using
287 transmission electron microscopy (Zbinden *et al.*, 2008). For the first time we
288 confirmed it with the typical circular positive FISH signal (Duperron *et al.*,
289 2005) with both the GAM42a probe and the LBI32/130 probe (Table 2, Fig. 2c).
290 On the Rainbow site, these methanotrophic like bacteria were clearly at the basis
291 of long filaments affiliated to *Epsilonproteobacteria*, directly fixed on the *R.*
292 *exoculata* tissues (LB and Sc) (Fig. S1). This specific localization seemed to
293 confirm that the type I methanotrophic *Gammaproteobacteria* were not
294 opportunistic. This morphology was observed only associated with Rainbow
295 juveniles and adults, whatever the moult stage. The other phylogenetic groups
296 (Table 1) were not detected in the gill chamber (using FISH analyses, Table 2).

297 II). Eggs – SEM and semi-thin observations showed the presence of a mat
298 of thin rod-shaped bacteria (around 2.5 μm length and 0.3 μm diameter) settled
299 on the egg surface for the majority of eggs observed (Fig. 1c, d, e). This
300 microbial mat hybridized only with the GAM42a probe, but no methanotrophic-
301 like bacteria was revealed by FISH analyses (Fig. 2d). TEM observations
302 confirmed the presence of bacteria embedded in a mucus covering the eggs (Fig.
303 1f) and some had intracytoplasmic membranes like type I methanotroph (Fig.
304 1g). They were smaller (1 μm) than the one observed on the Rainbow adult
305 shrimps (2 μm). No bacteria were observed inside the eggs (TEM and FISH).

306 III). Larvae – larvae used in this study had just hatched (Fig.1b) and were
307 still associated to their egg (Fig. 1a) (Fig. 4). SEM and FISH observations
308 showed no obvious bacterial mats on the larvae itself, but only single cells. No
309 bacteria were observed inside the larvae gill chamber (TEM and FISH).
310 Molecular surveys were therefore not undertaken on larvae alone, but on larvae
311 and its egg (hatched egg).

312 **Bacterial diversity (16S rRNA) along the *R. exoculata* life cycle.**

313 Diversity studies using PCR amplification and cloning are known to
314 underestimate genetic diversity because of faster amplification of some
315 sequences and bias both in amplification and cloning (Qiu *et al.*, 2001).
316 Moreover, sampling methods introduce additional biases (Bent and Forney,
317 2008). Clone libraries obtained in this study can therefore be considered only

318 partially quantitative. As all experiments were performed using the same
319 protocols, they can nevertheless be compared. Moreover FISH analyses
320 confirmed libraries diversity. Phylogenetic diversity along the *R. exoculata* life
321 cycle was completed using rarefaction analyses and diversity indices (Fig. S2,
322 Table S1). A total of 11 bacterial 16S rRNA gene clone libraries were analyzed,
323 corresponding to 817 clone sequences (Table 1). *Epsilonproteobacteria* and
324 *Gammaproteobacteria* dominated all the clone libraries (Table 1). This was
325 consistent with recent studies (Zbinden *et al.*, 2008; Petersen *et al.*, 2009; Hügler
326 *et al.*, 2011). *Deltaproteobacteria*, *Alphaproteobacteria*, *Betaproteobacteria* and
327 *Bacteroidetes* were poorly represented (Table 1), confirmed by the absence of
328 FISH signal. These sequences might represent opportunistic microorganisms
329 embedded in the mat covering the appendages. Nevertheless, recent Snake Pit
330 site study showing the recovery of one deltaproteobacterial phylotype in high
331 frequency, suggested that it might have a role in the epibiotic community
332 (Hügler *et al.*, 2011). The clone diversity coverage (Good's coverage) was high
333 for all clone libraries with an average of 93% (± 5) (Table S1) and the
334 rarefaction curves showed that the clone libraries correctly described the
335 epibiotic communities, excepted for hatched eggs library (Fig. S2).

336 In this study, *Epsilonproteobacteria* sequences were overwhelmingly
337 related to sequences usually retrieved from hydrothermal invertebrates (e.g.
338 *Cryosomallon squamiferum* (Goffredi *et al.*, 2004); *Alvinocaris longirostris*
339 (Tokuda *et al.*, 2008); *Shinkaia crosnieri* (unpublished); *Rimicaris exoculata*

340 gut (Zbinden *et al.*, 2003) and gill chamber (Polz and Cavanaugh, 1995;
341 Zbinden *et al.*, 2008; Petersen *et al.*, 2009) and also to the MAR environment
342 (Lost City (Brazelton *et al.*, 2006); Rainbow (Lopez-Garcia *et al.*, 2003); Snake
343 Pit (unpublished)) (Fig. 3A, B, Table S3). The main nine *Epsilonproteobacteria*
344 clusters fell within the “hydrothermal invertebrates associated epibionts” group
345 (Marine Group 1) (Fig. 3A). The closest cultivated relative was *Sulfurovum*
346 *lithotrophicum*, a sulfur-oxidizing chemolithoautotroph isolated from a
347 hydrothermal vent in the mid-Okinawa Trough (Inagaki *et al.*, 2004) (94%
348 similarity with *R. exoculata* RBR (AM412509)), Fig. 3B). Other
349 *Epsilonproteobacteria* sequences were affiliated to known genera:
350 *Thiomicrospira*, *Campylobacter*, *Arcobacter* and *Sulfospirillum* (Fig. 3A). The
351 three latter genera belong to the *Campylobacteraceae* family are known to
352 exhibit important metabolic diversity (including sulfur-oxidizing and reducing
353 bacteria). The closest *Thiomicrospira* species *T. denitrificans* (Fig. 3A, 89%
354 similarity with *R. exoculata* RBR (AM412516)) is an obligate chemolithotroph
355 oxidizing sulfide and thiosulfate, and is also a denitrifier (Muyzer *et al.*, 1995).
356 The Logachev and the Ashadze *Epsilonproteobacteria* related sequences
357 clustered together (Fig. 3B, cluster 3 and 6) but not with the Rainbow sequences
358 (Fig.3B, cluster 1, 2, 5, 7 and 8). Phylogenetic analyses showed that the same
359 epibiont sequences were retrieved all along the shrimp life cycle, from eggs to
360 adult on Logachev (Fig.3B, cluster 6 and 9). At the Rainbow site, some seawater
361 sequences (*R. exoculata* RBF (FR797932)) were almost identical (99.9%

362 similarity) to shrimp epibiont sequences (*R. exoculata* RBR (AM412509)) (Fig.
363 3B, cluster 7).

364 The *Gammaproteobacteria* were mostly affiliated to bacteria associated
365 with hydrothermal vent invertebrates (e.g. *C. squamiferum* and *K. hirsuta*
366 (Goffredi *et al.*, 2004); *Shinkaia crosnieri* (unpublished); *R. exoculata* (Zbinden
367 *et al.*, 2008)) (Fig. 3C, Table S3). The closest cultured relative to the cluster 1
368 *Gammaproteobacteria* epibionts (90.6% similarity) was *Leucothrix mucor*
369 (Grabovich *et al.*, 1999), a filamentous sulfur-oxidizer (Fig. 3C). The closest
370 cultivated relative to the cluster 2 *Gammaproteobacteria* epibionts (92.5%
371 similarity) was *Methylomonas methanica* (Costello and Lidstrom, 1999), a rod-
372 shaped methanotrophic bacterium (Fig. 3C).

373 All adult, juvenile and seawater libraries were dominated by the
374 *Epsilonproteobacteria* related sequences (Table 1). *Epsilonproteobacteria*
375 sequences dominated Logachev grey, Rainbow light red and Ashadze black
376 moult stages libraries compared to others (Table 1). The *Gammaproteobacteria*
377 were more represented in the Rainbow red moult library (Table 1).

378 Eggs and hatched eggs clone libraries distribution at Logachev were
379 clearly different compared to the adult, juvenile and seawater libraries (Table 1).
380 They were dominated by sequences related to the *Gammaproteobacteria* (Table
381 1), confirmed by FISH observations (Fig. 2d). For cluster 1, most of eggs and
382 hatched eggs sequences were closely related (99% similarity) to a *Shinkaia*

383 *crosnieri* epibiont (Fig.3C). For cluster 2, eggs and hatched eggs sequences were
384 closely related to *Methylomonas methanica* (Fig. 4).

385 Discussion

386 **Female behavior and life cycle.**

387 Until now, there was no report of *R. exoculata* females carrying eggs
388 inside the shrimp aggregates close to the hydrothermal chimney walls at the
389 MAR vent sites. One assumption was that gravid females were not inside the
390 aggregates to avoid damaging the eggs (Vereshchaka *et al.*, 1998), but only few
391 gravid shrimp have been observed around the MAR vent sites (Tyler and
392 Young, 1999). During the Serpentine cruise, gravid *R. exoculata* females were
393 observed and collected from aggregates at the Logachev vent chimney Irina II.
394 For the first time hatched eggs with larvae were collected, improving the
395 knowledge about the shrimp life cycle (Fig. 4). This cruise was held earlier in
396 the season (March) than others did (from May to November). The small size and
397 the composition (rich in lipids) of *R. exoculata* eggs could indicate short
398 embryonic development with larvae hatching at an early stage and undergoing a
399 relatively long planktotrophic period (Llodra *et al.*, 2000). *R. exoculata* could
400 thus exhibit seasonal reproduction, in which larvae hatch in early spring and
401 undertake an as yet unspecified period of planktotrophic development in the
402 water column. The lack of year-round data (absence of specimen between larvae
403 and 1.2 cm juvenile) made it difficult to conclude on the full life cycle of this
404 shrimp (Fig. 4). All eggs on a given female were at the same maturity stage, but

405 the stage differed from one female to another. This indicated that they were not
406 sexually mature at the same time, and that reproductive period would be longer
407 than the egg development duration. Eggs were still associated with the gravid
408 females when the hatching occurred so only mature larvae would be released.
409 To evaluate the egg development duration, pressured incubator (IPOCAMP™)
410 maintenance of gravid females would be necessary.

411 **Epibiont diversity and acquisition.**

412 Some epibiont sequences were retrieved all along the shrimp life cycle
413 (Fig. 3B, cluster 6 and 9; Fig. 3C, cluster 1 and 2). This result suggested a high
414 specificity and the occurrence of an acute recognition mechanism such as in
415 nematode ectosymbioses (Nussbaumer *et al.*, 2004). Moreover, molecular
416 surveys indicated a bacterial community switch occurring between the first
417 stages of the *R. exoculata* life cycle (egg and hatched egg libraries dominated by
418 the *Gammaproteobacteria*) and latter stages (juvenile / adult libraries dominated
419 by the *Epsilonproteobacteria*) (Table 1), confirmed by FISH observations (Fig.
420 2a, b versus d). These results reinforced the occurrence of a complex stable
421 symbiosis in *R. exoculata* with the same *Gamma* and *Epsilonproteobacteria*
422 related sequences and further showed that symbiont phylotypes
423 representativeness could vary according to the life stage of the host.
424 Observations highlighted the presence of colorless mucus-like material
425 surrounding the eggs. Mucus could be a „scaffolding“ that provides anchorage
426 and protection for the eggs (Davies and Viney, 1998), while epibionts embedded

427 in the mucus could have a protective role in detoxication and also against
428 potential pathogens (e.g. bacteria and fungi). This was the case for epibiotic
429 bacteria associated with the *Homarus americanus* embryo which produce
430 substances inhibiting pathogenic fungi growth (Gilturmes and Fenical, 1992).
431 Bacteria within the gill chamber could have roles, such as detoxication or
432 nutrition for the host (Zbinden *et al.*, 2004, 2008).

433 Ashadze and Logachev sequences clustered together (Fig. 3B, cluster 3
434 and 6) which might be explained by the very close proximity between these two
435 sites (Fabri *et al.*, 2010). A recent study showed a significant correlation
436 between genetic (16S rRNA) and geographic distances for *R. exoculata*
437 epibionts along the MAR (Petersen *et al.*, 2009). The depth could also explain
438 the clustering with the possible depth limit of 3000 m previously proposed
439 (Priede *et al.*, 2006). Some *Epsilon* and *Gammaproteobacteria* sequences
440 retrieved from the Rainbow seawater sample were closely related (99%
441 similarity) to epibiont sequences from the gill chamber of shrimps from the
442 same site (Fig. 3B cluster 1, 5 and 7; Fig. 3C cluster 1). All of these results
443 would indicate the existence of horizontal (environmental) transmission for the
444 shrimp cephalothorax epibionts. Epibionts associated to egg mucus could also
445 be a result of vertical transmission (from mother to offspring) through mucus
446 secretion (Mira and Moran, 2002). Vertical transmission usually implies
447 internalization of symbionts inside the egg or in oviducts (Bright and
448 Bulgheresi, 2010). But, microscopic observations (SEM, TEM and FISH)

449 showed that (I) there were no active bacteria inside the eggs, but only associated
450 with their outer surface (Fig. 1c), and (II) no bacterial mat was observed
451 associated with the young larvae just after hatching. The egg mucus interface
452 probably facilitated attraction, accumulation and host recognition of epibionts
453 for horizontal transmission. This epibiont transmission pathway is in adequacy
454 with the large colonization of the MAR by *R. exoculata* because horizontal
455 transmission is supposed to promote dispersal compared to vertical transmission
456 (Chaston and Goodrich-Blair, 2010). In terms of evolution, it was suggested that
457 episymbiosis represents a more primitive stage than endosymbiosis (Dubilier *et*
458 *al.*, 2008). The internalization of symbionts would then represent the final step
459 of the association. Nevertheless, a recent study based on 16S rRNA analyses
460 demonstrated that bathymodiolin epibionts were not ancestral to bathymodiolin
461 endosymbionts (Duperron *et al.*, 2009). These authors suggested that the
462 location of symbionts was not always a conserved trait and that both the host
463 and the symbiotic bacteria were more versatile in their ability to establish
464 associations than previously assumed.

465 It should be noted that only three gravid females were used for
466 phylogenetic studies (Table S2). More specimens of the first stages of the
467 shrimp life cycle (notably free larvae at each developmental stage) are necessary
468 for complementary analyses.

469

470

471 **The methanotrophic metabolism hypothesis**

472 Methanotrophic symbionts use methane as both an electron donor and a
473 carbon source, with oxygen as the final electron acceptor. These symbionts have
474 been described in deep-sea hydrothermal vents and cold seeps, where methane
475 co-occurs with oxygen (Petersen and Dubilier, 2009). *In situ* observations
476 showed that *R. exoculata* lives in the mixing zone between reduced
477 hydrothermal fluid (containing methane at Rainbow and Logachev) and
478 oxidized ambient seawater. Methane oxidation metabolism was previously
479 suspected (Zbinden *et al.*, 2008). To our knowledge, all 16S rRNA sequences of
480 methanotrophic symbionts from marine invertebrates belong to a single
481 monophyletic lineage within the *Gammaproteobacteria* phyla related to type I
482 methanotrophs. These bacteria are coccoid and have a concentric stacking of
483 intracytoplasmic membranes, where the methanotrophic enzymes are located
484 (Hanson and Hanson, 1996). These membranes probably push back the cellular
485 material (including ribosomes) to the cell periphery, explaining the characteristic
486 circular FISH hybridization signal (Fig. 2c). In this study, we have shown using
487 molecular and microscopic approaches, the presence of active type I
488 methanotrophic bacteria occurring in the cephalothorax of the Rainbow
489 specimens (Fig. 2c and Fig. 3C, cluster 2) and located at the base of the
490 filamentous bacteria (Fig. S1). This result was congruent with the fluid
491 composition of this site, which is highly enriched in methane (Charlou *et al.*,

492 2002) and confirmed a previous study (Zbinden *et al.*, 2008). Regarding the
493 eggs, TEM observations revealed methanotrophs shaped bacteria associated
494 with their membrane (Fig. 1g) and sequences affiliated to the methanotrophic
495 cluster were retrieved (Fig. 3C, cluster 2). According to their small size, these
496 cells might then be dormant, which could explain the absence of FISH signal.
497 Logachev, like Rainbow, is enriched in methane (Schmidt *et al.*, 2007) (Table
498 S2). Therefore, methanotrophy might also occur at this site, but at a lower
499 activity level. No methanotrophic related sequence has been retrieved in the
500 Rainbow seawater sample. This could be due to a PCR bias, the low number of
501 sequences treated or could indicate they were poorly present as free living
502 forms. Taken altogether, our results indicated the presence of methanotrophic
503 bacteria associated with *R. exoculata* (eggs and adults) in two sites, reinforcing
504 the symbiosis hypothesis. This could therefore be the first description of an
505 epibiotic association between methanotrophic bacteria and hydrothermal vent
506 crustaceans.

507 **Conclusion**

508 By describing the young larva just after hatching (Fig. 4), we improved
509 the knowledge of the *R. exoculata* life cycle. Nevertheless, the dispersion and
510 recruitment of *R. exoculata* along the MAR vent sites still unknown (Fig. 4).
511 Like larval dispersion, symbiont transmission is obviously an integral factor
512 influencing colonization efficiency (Teixeira *et al.*, 2011). Our results indicated

513 a possible horizontal transmission for the gill chamber epibionts of *R. exoculata*
514 that could explain colonization along the MAR.

515 We have also described for the first time epibiotic communities associated
516 with eggs and different stages from adults, and highlighted a community switch
517 between *Gamma* and *Epsilonproteobacteria*. By coupling molecular biology and
518 microscopic approaches we have demonstrated the occurrence of type I
519 methanotrophic *Gammaproteobacteria*, one of the three metabolisms (iron,
520 sulfur, and methane oxidation) expected to occur in the gill chamber (Zbinden *et*
521 *al.*, 2008). Our results indicated that the epibiotic community was globally
522 conserved along the MAR. We suggest that the phylotype relative abundance
523 and the activity of the epibionts could vary according to the shrimp life stage
524 and to the geochemical environment, reinforcing the symbiotic hypothesis.
525 Future investigations will focus on identification (by PCR and RT-PCR) of
526 functional genes implied in these different metabolisms. Deeper sequencing
527 using high throughput sequencing technologies would be useful to exhaust the
528 diversity. Finally, more sampling in the aggregates and in the water column will
529 be necessary to complete the shrimp life cycle, as well as incubation
530 experiments using gravid females.

531 Acknowledgments

532 The authors wish to thank Y. Fouquet and F. Gaill, respectively chief
533 scientists of the Serpentine and MOMARDREAM-Naut cruises, as well as the
534 captain and crew of the *Pourquoi pas ?* and Nautile / Victor teams. Thanks to M.

535 Perennou and S. Romac from the „Plateforme Biogenouest“ for sequencing
536 work. TEM was undertaken by the Service de Microscopie Electronique, IFR 83
537 de Biologie Integrative – CNRS / Paris VI. We also gratefully thank I. Probert
538 and M. Segonzac for their advice and comment. This work was supported by
539 Ifremer, CNRS, Brest Metropole Oceane, GDR ECCHIS, ANR Deep Oases.

540 **Supplementary information is available at ISME’s website.**

541 References

- 542 Altschul SF, Gish W, Miller W, Myers EW, Lipman DJ. (1990). Basic Local Alignment Search Tool.
543 *J Mol Biol* **215**: 403-410.
544
- 545 Amann RI, Krumholz L, Stahl DA. (1990). Fluorescent-Oligonucleotide Probing of Whole Cells for
546 Determinative, Phylogenetic, and Environmental Studies in Microbiology. *J Bacteriol* **172**: 762-770.
547
- 548 Bates AE, Harmer TL, Roeselers G, Cavanaugh CM. (2011). Phylogenetic Characterization of
549 Episymbiotic Bacteria Hosted by a Hydrothermal Vent Limpet (Lepetodrilidae, Vetigastropoda). *Biol*
550 *Bull* **220**: 118-127.
551
- 552 Bent SJ, Forney LJ. (2008). The tragedy of the uncommon: understanding limitations in the analysis of
553 microbial diversity. *ISME J* **2**: 689-695.
554
- 555 Brazelton WJ, Schrenk MO, Kelley DS, Baross JA. (2006). Methane- and sulfur-metabolizing
556 microbial communities dominate the Lost City hydrothermal field ecosystem. *Appl Environ Microbiol*
557 **72**: 6257-6270.
558
- 559 Bright M, Bulgheresi S. (2010). A complex journey: transmission of microbial symbionts. *Nature Rev*
560 *Microbiol* **8**: 218-230.
561
- 562 Casanova B, Brunet M, Segonzac M. (1993). Impact of bacterial epibiosis on functional-morphology
563 of shrimp associated with the Mid-Atlantic hydrothermal conditions. *Cah Biol Mar* **34**: 573-588.
564
- 565 Charlou JL, Donval JP, Fouquet Y, Jean-Baptiste P, Holm N. (2002). Geochemistry of high H₂ and
566 CH₄ vent fluids issuing from ultramafic rocks at the Rainbow hydrothermal field (36°14 ' N, MAR).
567 *Chem Geol* **191**: 345-359.
568
- 569 Chaston J, Goodrich-Blair H. (2010). Common trends in mutualism revealed by model associations
570 between invertebrates and bacteria. *FEMS Microbiol Rev* **34**: 41-58.
571
- 572 Copley CEA, Tyler PA, Varney MS. (1998). Lipid profiles of hydrothermal vent shrimps. *Cah Biol*
573 *Mar* **39**: 229-231.
574
- 575 Corbari L, Zbinden M, Cambon-Bonavita MA, Gaill F, Compère P. (2008). Bacterial symbionts and
576 mineral deposits in the branchial chamber of the hydrothermal vent shrimp *Rimicaris exoculata*:
577 relationship to moult cycle. *Aquat Biol* **1**: 225–238.

578
579 Costello AM, Lidstrom ME. (1999). Molecular Characterization of Functional and Phylogenetic
580 Genes from Natural Populations of Methanotrophs in Lake Sediments. *Appl Environ Microbiol* **65**:
581 5066–5074.
582
583 Davies JM, Viney C. (1998). Water-mucin phases: conditions for mucus liquid crystallinity.
584 *Thermochim Acta* **315**: 39-49.
585
586 Desbruyères D, Biscoito M, Caprais JC, Colaço A, Comtet T, Crassous P *et al.* (2001). Variations in
587 deep-sea hydrothermal vent communities on the Mid-Atlantic Ridge near the Azores plateau. *Deep-*
588 *Sea Res I* **48**: 1325-1346.
589
590 Douville E, Charlou JL, Oelkers EH, Bienvenu P, Colon CFJ, Donval JP *et al.* (2002). The Rainbow
591 vent fluids (36°14'N, MAR): the influence of ultramafic rocks and phase separation on trace metal
592 content in Mid-Atlantic Ridge hydrothermal fluids. *Chem Geol* **184**: 37-48.
593
594 Dubilier N, Bergin C, Lott C. (2008). Symbiotic diversity in marine animals: the art of harnessing
595 chemosynthesis. *Nature Rev Microbiol* **6**: 725-740.
596
597 Duperron S, Nadalig T, Caprais JC, Sibuet M, Fiala-Medioni A, Amann R *et al.* (2005). Dual
598 symbiosis in a Bathymodiolus sp mussel from a methane seep on the gabon continental margin
599 (southeast Atlantic): 16S rRNA phylogeny and distribution of the symbionts in gills. *Appl Environ*
600 *Microbiol* **71**: 1694-1700.
601
602 Duperron S, Lorion J, Samadi S, Gros O, Gaill F. (2009). Symbioses between deep-sea mussels
603 (Mytilidae: Bathymodiolinae) and chemosynthetic bacteria: diversity, function and evolution. *C R*
604 *Biologies* **332**: 298-310.
605
606 Duperron S, De Beer D, Zbinden M, Boetius A, Schipani V, Kahil N, Gaill F. (2009). Molecular
607 characterization of bacteria associated with the trophosome and the tube of *Lamellibrachia* sp., a
608 siboglinid annelid from cold seeps in the eastern Mediterranean. *FEMS Microbiol Ecol* **69**: 395-409.
609
610 Durand L, Zbinden M, Cuff-Gauchard V, Duperron S, Roussel EG, Shillito B *et al.* (2010). Microbial
611 diversity associated with the hydrothermal shrimp *Rimicaris exoculata* gut and occurrence of a
612 resident microbial community. *FEMS Microbiol Ecol* **71**: 291-303.
613
614 Fabri MC, Bargain A, Briand P, Gebruk A, Fouquet Y, Morineaux M *et al.* (2010). The hydrothermal
615 vent community of a new deep-sea field, Ashadze-1, 12°58'N on the Mid-Atlantic Ridge. *J Mar Biol*
616 *Assoc UK*: 1-13.
617
618 Felsenstein J. (1985). Confidence limits on phylogenies: an approach using the bootstrap. *Evolution*
619 **39**: 783-791.
620
621 Galtier N, Gouy M, Gautier C. (1996). SEAVIEW and PHYLO_WIN: Two graphic tools for sequence
622 alignment and molecular phylogeny. *Comput Appl Biosci* **12**: 543-548.
623
624 Gebruk AV, Pimenov NV, Savvichev AS. (1993). Feeding specialization of bresilid shrimps in the
625 TAG site hydrothermal community. *Mar Ecol Prog Ser* **98**: 247-253.
626
627 Giltunes MS, Fenical W. (1992). Embryos of *Homarius americanus* are protected by epibiotic
628 bacteria. *Biol Bull* **182**: 105-108.
629
630 Goffredi SK, Waren A, Orphan VJ, Van Dover CL, Vrijenhoek RC. (2004). Novel forms of structural
631 integration between microbes and a hydrothermal vent gastropod from the Indian Ocean. *Appl Environ*
632 *Microbiol* **70**: 3082-3090.

633
634 Goffredi SK. (2010) Indigenous ectosymbiotic bacteria associated with diverse hydrothermal vent
635 invertebrates. *Environ Microbiol Reports* **2**:479-488.
636
637 Good IJ. (1953). The population frequencies of species and the estimation of population parameters.
638 *Biometrika* **40**: 237-264.
639
640 Grabovich MY, Muntyan MS, Lebedeva VY, Ustiyani VS, Dubinina GA. (1999). Lithoheterotrophic
641 growth and electron transfer chain components of the filamentous gliding bacterium *Leucothrix mucor*
642 DSM 2157 during oxidation of sulfur compounds. *FEMS Microbiol Lett* **178**: 155-161.
643
644 Hanson RS, Hanson TE. (1996). Methanotrophic Bacteria. *Microbiol Rev* **60**: 439-471.
645
646 Hügler M, Petersen JM, Dubilier N, Imhoff JF, Sievert SM. (2011). Pathways of carbon and energy
647 metabolism of the epibiotic community associated with the deep-sea hydrothermal vent shrimp
648 *Rimicaris exoculata*. *PLoS Biol* (in press).
649
650 Inagaki F, Takai K, Nealson KH, Horikoshi K. (2004). *Sulfurovum lithotrophicum* gen. nov., sp nov.,
651 a novel sulfur-oxidizing chemolithoautotroph within the e-Proteobacteria isolated from Okinawa
652 Trough hydrothermal sediments. *Int J Syst Evol Microbiol* **54**: 1477-1482.
653
654 Komai T, Segonzac M. (2008). Taxonomic review of the hydrothermal vent shrimp genera *Rimicaris*
655 *Williams & Rona* and *Chorocaris* Martin & Hessler (Crustacea : Decapoda : Caridea :
656 *Alvinocarididae*). *J Shellfish Res* **27**: 21-41.
657
658 Lane D. (1991). 16S/23S rRNA sequencing. *Nucleic Acid Techn Bact Syst* **1**: 115-176.
659
660 Lin X, Wakeham SG, Putnam IF, Astor YM, Scranton MI, Chistoserdov AY *et al.* (2006).
661 Comparison of Vertical Distributions of Prokaryotic Assemblages in the Anoxic Cariaco Basin and
662 Black Sea by Use of Fluorescence In Situ Hybridization. *Appl Environ Microbiol* **72**: 2679-2690.
663
664 Llodra ER, Tyler PA, Copley JTP. (2000). Reproductive biology of three caridean shrimp, *Rimicaris*
665 *exoculata*, *Chorocaris chacei* and *Mirocaris fortunata* (Carudea : Decapoda), from hydrothermal
666 vents. *J Mar Biol Assoc UK* **80**: 473-484.
667
668 Lopez-Garcia P, Duperron S, Philippot P, Foriel J, Susini J, Moreira D. (2003). Bacterial diversity in
669 hydrothermal sediment and epsilon proteobacterial dominance in experimental microcolonizers at the
670 Mid-Atlantic Ridge. *Environ Microbiol* **5**: 961-976.
671
672 Loy A, Lehner A, Lee N, Adamczyk J, Meier H, Ernst J *et al.* (2002). Oligonucleotide microarray for
673 16S rRNA gene-based detection of all recognized lineages of sulfate-reducing prokaryotes in the
674 environment. *Appl Environ Microbiol* **68**: 5064-5081.
675
676 Manz W, Amann R, Ludwig W, Vancanneyt M, Schleifer KH. (1996). Application of a suite of 16S
677 rRNA-specific oligonucleotide probes designed to investigate bacteria of the phylum cytophaga-
678 flavobacter-bacteroides in the natural environment. *Microbiology* **142**: 1097-1106.
679
680 Manz W, Amann R, Ludwig W, Wagner M, Schleifer KH. (1992). Phylogenetic oligodeoxynucleotide
681 probes for the major subclasses of *Proteobacteria*: problems and solutions. *Syst Appl Microbiol* **15**:
682 593-600.
683
684 Mira A, Moran NA. (2002). Estimating population size and transmission bottlenecks in maternally
685 transmitted endosymbiotic bacteria. *Microbial Ecol* **44**: 137-143.
686

687 Muyzer G, Teske A, Wirsen CO, Jannasch HW. (1995). Phylogenetic relationships of *Thiomicrospira*
688 species and their identification in deep-sea hydrothermal vent samples by denaturing gradient gel
689 electrophoresis of 16S rDNA fragments. *Arch Microbiol* **164**: 165-172.
690

691 Nussbaumer AD, Bright M, Baranyi C, Beisser CJ, Ott JA. (2004). Attachment mechanism in a highly
692 specific association between ectosymbiotic bacteria and marine nematodes. *Aquat Microb Ecol* **34**:
693 239-246.
694

695 Petersen JM, Ramette A, Lott C, Cambon-Bonavita MA, Zbinden M, Dubilier N. (2009). Dual
696 symbiosis of the vent shrimp *Rimicaris exoculata* with filamentous gamma- and epsilonproteobacteria
697 at four Mid-Atlantic Ridge hydrothermal vent fields. *Environ Microbiol* **12**: 2204-2218.
698

699 Petersen JM, Dubilier N. (2009). Methanotrophic symbioses in marine invertebrates. *Environ*
700 *Microbiol* **1**: 319-335.
701

702 Polz MF, Robinson JJ, Cavanaugh CM, Van Dover CL. (1998). Trophic ecology of massive shrimp
703 aggregations at a Mid-Atlantic Ridge hydrothermal vent site. *Limnol Oceanogr* **43**: 1631-1638.
704

705 Polz MF, Cavanaugh CM. (1995). Dominance of one bacterial phylotype at a Mid-Atlantic Ridge
706 hydrothermal vent site. *Proc Natl Acad Sci USA* **92**: 7232-7236.
707

708 Pond DW, Segonzac M, Bell MV, Dixon DR, Fallick AE, Sargent JR. (1997). Lipid and lipid carbon
709 stable isotope composition of the hydrothermal vent shrimp *Mirocaris fortunata*: evidence for
710 nutritional dependence on photosynthetically fixed carbon. *Mar Ecol Prog Ser* **157**: 221-231.
711

712 Pond DW, Gebruk A, Southward EC, Southward AJ, Fallick AE, Bell MV *et al.* (2000). Unusual fatty
713 acid composition of storage lipids in the bresilioid shrimp *Rimicaris exoculata* couples the photic zone
714 with MAR hydrothermal vent sites. *Mar Ecol Prog Ser* **198**: 171-179.
715

716 Priede IG, Froese R, Bailey DM, Bergstad OA, Collins MA, Dyb JE *et al.* (2006). The absence of
717 sharks from abyssal regions of the world's oceans. *Proceedings of the Royal Society B: Biological*
718 *Sciences* **273**: 1435-1441.
719

720 Qiu XY, Wu LY, Huang HS, McDonel PE, Palumbo AV, Tiedje JM *et al.* (2001). Evaluation of PCR-
721 generated chimeras: Mutations, and heteroduplexes with 16S rRNA gene-based cloning. *Appl Environ*
722 *Microbiol* **67**: 880-887.
723

724 Ravensschlag K, Sahn K, Pernthaler J, Amann R. (1999). High Bacterial Diversity in Permanently
725 Cold Marine Sediments. *Appl Environ Microbiol* **65**: 3982-3989.
726

727 Rieley G, Van Dover CL, Hedrick DB, Eglinton G. (1999). Trophic ecology of *Rimicaris exoculata*: a
728 combined lipid abundance stable isotope approach. *Mar Biol* **133**: 495-499.
729

730 Ruehland C, Dubilier N. (2010). Gamma- and epsilonproteobacterial ectosymbionts of a shallow-
731 water marine worm are related to deep-sea hydrothermal vent ectosymbionts. *Environ Microbiol*
732 **12**:2312-2326.
733

734 Saitou N, Nei M. (1987). The neighbor-joining method: a new method for reconstructing phylogenetic
735 trees. *Mol Biol Evol* **4**: 406-425.
736

737 Schloss PD, Handelsman J. (2005). Introducing DOTUR, a Computer Program for Defining
738 Operational Taxonomic Units and Estimating Species Richness. *Appl Environ Microbiol* **71**: 1501-
739 1506.
740

741 Schmidt C, Le Bris N, Gaill F. (2008). Interactions of deep-sea vent invertebrates with their
742 environment: The case of *Rimicaris exoculata*. *J Shellfish Res* **27**: 79-90.
743

744 Schmidt K, Koschinsky A, Garbe-Schönberg D, de Carvalho LM, Seifert R. (2007). Geochemistry of
745 hydrothermal fluids from the ultramafic-hosted Logatchev hydrothermal field, 15°N on the Mid-
746 Atlantic Ridge: Temporal and spatial investigation. *Chem Geol* **242**: 1-21.
747

748 Segonzac M. (1992). The hydrothermal vent communities of Snake Pit area (Mid-Atlantic Ridge,
749 23°N, 3480 m) - Megafaunal composition and distribution. *C R Acad Sci Paris, Life Sci* **314**: 593-600.
750

751 Segonzac M, Saint-Laurent M, Casanova B. (1993). Enigma of the trophic adaptation of the shrimp
752 Alvinocarididae in hydrothermal areas along the Mid-Atlantic Ridge. *Cah Biol Mar* **34**: 535-571.
753

754 Shillito B, Le Bris N, Gaill A, Rees JF, Zal F. (2004). First access to live *Alvinella*. *High Pressure Res*
755 **24**: 169-172.
756

757 Stahl D, Amann R. (1991). Development and application of nucleic acid probes. *Nucleic Acid Techn*
758 *Bact Syst*: pp. 205-247. Wiley Inc., New York.
759

760 Teixeira S, Cambon-Bonavita MA, Serrão EA, Desbruyères D, Arnaud-Haond S. (2011). Recent
761 population expansion and connectivity in the hydrothermal shrimp *Rimicaris exoculata* along the Mid-
762 Atlantic Ridge. *J Biogeography* **38**: 564-574.
763

764 Thompson JD, Higgins DG, Gibson TJ. (1994). Clustalw: improving the sensitivity of progressive
765 multiple sequence alignment through sequence weighting, position-specific gap penalties and weight
766 matrix choice. *Nucleic Acids Res* **22**: 4673-4680.
767

768 Tokuda G, Yamada A, Nakano K, Arita N, Yamasaki H. (2006). Occurrence and recent long-distance
769 dispersal of deep-sea hydrothermal vent shrimps. *Biol Lett* **2**: 257-260.
770

771 Tokuda G, Yamada A, Nakano K, Arita NO, Yamasaki H. (2008). Colonization of *Sulfurovum* sp on
772 the gill surfaces of *Alvinocaris longirostris*, a deep-sea hydrothermal vent shrimp. *Mar Ecol* **29**: 106-
773 114.
774

775 Tyler PA, Young CM. (1999). Reproduction and dispersal at vents and cold seeps. *J Mar Biol Assoc*
776 *UK* **79**: 193-208.
777

778 Van Dover CL, Fry B, Grassle JF, Humphris S, Rona PA. (1988). Feeding biology of the shrimp
779 *Rimicaris exoculata* at hydrothermal vents on the Mid-Atlantic Ridge. *Mar Biol* **98**: 209-216.
780

781 Williams AB, Rona PA. (1986). Two New Caridean Shrimps (Bresiliidae) from a Hydrothermal Field
782 on the Mid-Atlantic Ridge. *J Crust Biol* **6**: 446-462.
783

784 Zbinden M, Cambon-Bonavita MA. (2003). Occurrence of Deferribacterales and Entomoplasmatales
785 in the deep-sea Alvinocarid shrimp *Rimicaris exoculata* gut. *FEMS Microbiol Ecol* **46**: 23-30.
786

787 Zbinden M, Shillito B, Le Bris N, Villardi de Montlaur C, Roussel E, Guyot F, Gaill F, Cambon-
788 Bonavita MA. (2008). New insights on the metabolic diversity among the epibiotic microbial
789 community of the hydrothermal shrimp *Rimicaris exoculata*. *J Exp Mar Biol Ecol* **359**: 131-140.
790

791 Zbinden M, Le Bris N, Gaill F, Compère P. (2004). Distribution of bacteria and associated minerals in
792 the gill chamber of the vent shrimp *Rimicaris exoculata* and related biogeochemical processes. *Mar*
793 *Ecol Prog Ser* **284**: 237-251.
794
795

796

Table and Figure legends.

797 Table 1: Clone library results (based on partial 16S rRNA sequences). The main

798 phylogenetic group per sample is shown in bold (*by Zbinden *et al.*, 2008).

799

Phylogenetics groups	Logachev						Rainbow				Ashadze	Total
	Eggs	Hatched eggs	Juvenile	White moult	Grey moult	Black moult	White moult	Light Red moult	Red moult*	Hydrothermal fluid	Black moult	
<i>Alphaproteobacteria</i>	3	2					2	1	3			11
<i>Betaproteobacteria</i>							4	1				5
<i>Gammaproteobacteria</i>	53	30	1			1	10	1	25	5		126
<i>Deltaproteobacteria</i>	1	2	3	15		21			3	1		46
<i>Epsilonproteobacteria</i>	6	3	50	71	84	83	38	67	45	54	95	596
<i>Bacteroidetes</i>	4	7	7	1		3	5	1		4	1	33
Total	67	44	61	87	84	108	59	71	76	64	96	817

819

818

817

816

815

814

813

812

811

810

809

808

807

806

805

804

803

802

801

800

Table 2: Fluorescent probes (The probes sequences have been compared using BLAST to our sequences to check their specificity and determined their mismatches).

Specificity	Probe name	Sequence (5'-3')	Fluorescent dye	% Formamide	References
<i>Archaea</i>	Arch915	GTGCTCCCCCGCCAATTCCT	Cy3	10-20-30	Stahl and Amann, 1991
<i>Eubacteria</i>	Eub338	GCTGCCTCCCGTAGGAGT	Cy3 or Cy5 or ATTO488	10-20-30-40	Amann <i>et al.</i> , 1990
<i>Alphaproteobacteria</i>	ALF968	GGTAAGGTTCTGCGCGTT	Cy3	10-20-30-40	Manz <i>et al.</i> , 1992
<i>Betaproteobacteria</i>	BET42a	GCCTTCCCACATCGTTT	Cy3	10-20-30-40	Manz <i>et al.</i> , 1992
<i>Deltaproteobacteria</i>	DELTA495b	AGTTAGCCGGCGCTTCCT	Cy3	10-20-30-40	Loy <i>et al.</i> , 2002
<i>Gammaproteobacteria</i>	GAM42a	GCCTTCCCACATCGTTT	Cy3	10-20-30-40	Manz <i>et al.</i> , 1992
<i>Epsilonproteobacteria</i>	EPSY549	CAGTGATTCCGAGTAACG	Cy3	20-30	Lin <i>et al.</i> , 2006
<i>Bacteroidetes</i>	CF319	TGGTCCGTGTCTGAGTAC	ATTO488	10-20-30-40	Manz <i>et al.</i> , 1996
<i>Gammaproteobacteria R. exoculata</i> cephalothoracic clones	LB132/130	TCCTGGCTATCCCCCACTAC	ATTO488	10-20-30	Durand <i>et al.</i> , 2009

843

842

841

840

839

838

837

836

835

834

833

832

831

830

829

828

827

826

825

824

823

822

821

820

844 Figure 1: Microscopic observations of eggs and larvae (SEM : c, e ; TEM : f and
845 g).

846 a. *R. exoculata* eggs from Logachev. Scale bar = 500 μm .

847 b. *R. exoculata* larvae which just hatched from Logachev (manually
848 separated from egg). Scale bar = 200 μm .

849 c. Egg surface from Logachev covered by thin rod-shaped bacterial mat.

850 d. Egg thin-section from Logachev, showing bacterial mat (indicated with
851 dark arrows) on *R. exoculata* egg membrane. Scale bar = 10 μm .

852 e. Focus on picture c, showing thin rod-shaped bacterial mat.

853 f. Egg thin-section, showing thin rod-shaped bacteria (indicated with dark
854 arrows) on the egg membrane. Scale bar = 2 μm .

855 g. Methanotrophic like bacteria (with intracytoplasmic membranes, indicated
856 with a dark arrow) retrieved in the thin rod-shaped bacterial mat
857 associated with the egg membrane. Scale bar = 500 nm.

858 Figure 2: Fluorescence *in situ* hybridization.

859 a. Longitudinal view of Scaphognathite setae from Logachev black moult
860 shrimp with epibionts. *Gammaproteobacteria* (red) were hybridized with
861 GAM42a probe, *Epsilonproteobacteria* (green) were hybridized by
862 EPSY549 probe.

863 b. Transversal view of Scaphognathite setae from Logachev black moult
864 shrimp with epibionts. *Gammaproteobacteria* (red) were hybridized with

865 GAM42a probe, *Epsilonproteobacteria* (green) were hybridized by
866 EPSY549 probe.

867 c. Longitudinal view of Scaphognathite *setae* from Rainbow red moult
868 shrimp with epibionts. The methanotrophic Gamma symbionts (orange)
869 were hybridized with both LBI32/130 and GAM42a probes. The DAPI
870 stained are in blue.

871 d. Egg membrane (mb) with epibionts, (in) eggs content, (out) outer
872 environment. *Gammaproteobacteria* (red) were hybridized with GAM42a
873 probe. The DAPI stained are in blue, showing eukaryotic nucleus of the
874 egg.

875 Figure 3:16S rRNA phylogeny of the *Epsilonproteobacteria* (A and B,
876 calculated on 817 bp) and *Gammaproteobacteria* (C, calculated on 804 bp)
877 associated with the *R. exoculata* gill chamber. The robustness was tested using
878 500 bootstraps resampling of the tree calcuted using the Neighbor-Joining
879 algorithm with Kimura two-parameters correction matrix (only bootstrap values
880 over 70 are shown). Sequences names have been resumed as: AD, LG or RB for
881 Ashadze, Logachev or Rainbow specimens, respectively, and E, HE, J, W, G, B,
882 LR, R and F for Eggs, Hatched Eggs, Juvenile, White moult, Grey moult, Black
883 moult, Light Red moult, Red moult and Fluid, respectively, and finally the
884 numbers in brackets refer to the number assigned to each individual. Our clones
885 are shown in color.

886 A. Global tree representing the *R. exoculata* epsilon symbiont and their close
887 relatives.

888 B. Secondary tree showing the “Hydrothermal invertebrates associated
889 epibionts” (Marine Group 1) (see Fig. 3A). Black arrow indicates the first *R.*
890 *exoculata* epibiont sequence discovered in the Snake Pit site.

891 C: 16S rRNA phylogeny of the *Gammaproteobacteria* associated with *R.*
892 *exoculata* gill chamber

893 Figure 4: Partial *R. exoculata* life cycle completed by this study.

894

895

896

897

898

899

900

901

902

903

904

905

906

907

908

909

910

911

912

913

914

915

916



917

918

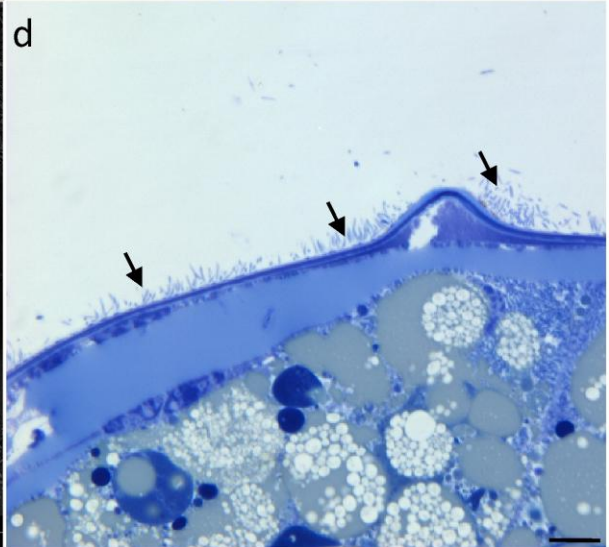
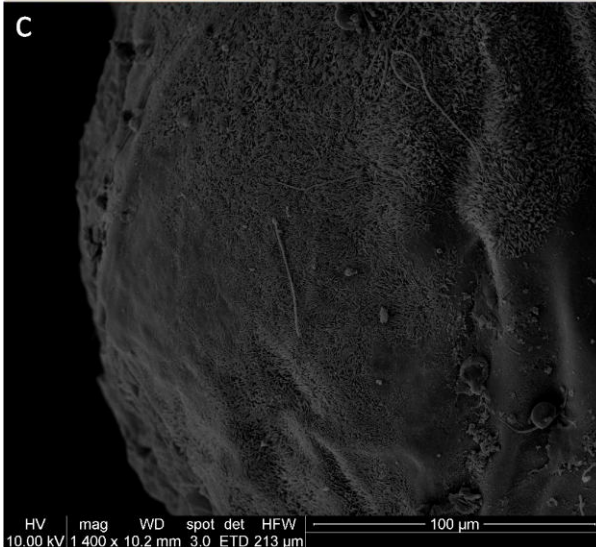
919

920

921

922

923



924

925

926

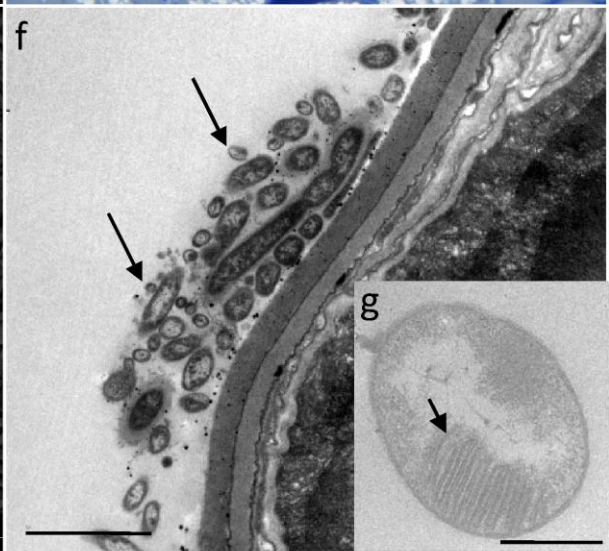
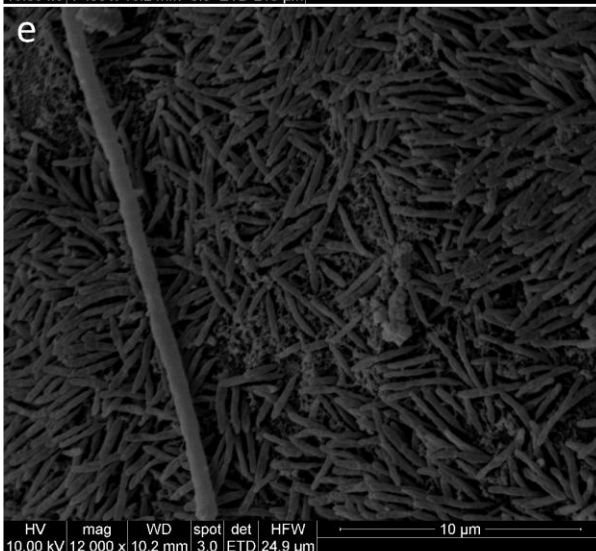
927

928

929

930

931



932

933

934

935

936

937

938

939

940

941

942

943

944

945

946

947

948

949

950

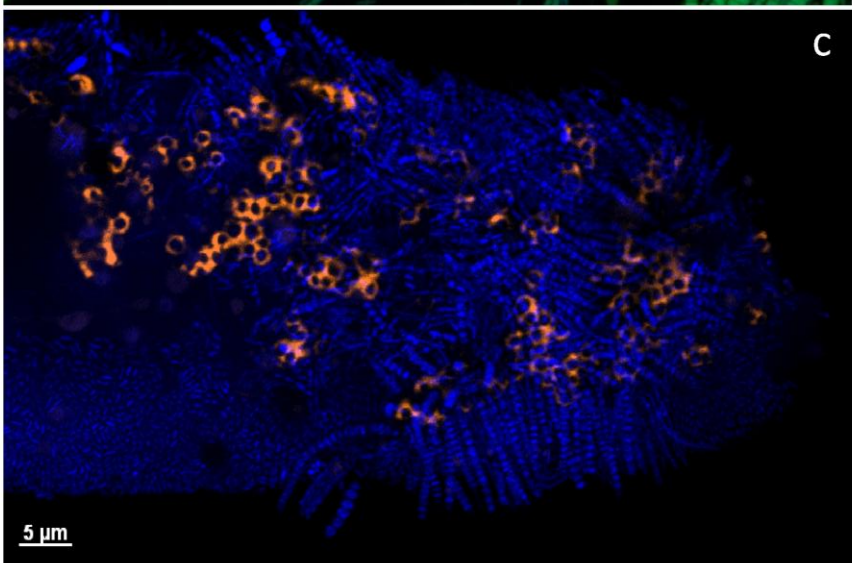
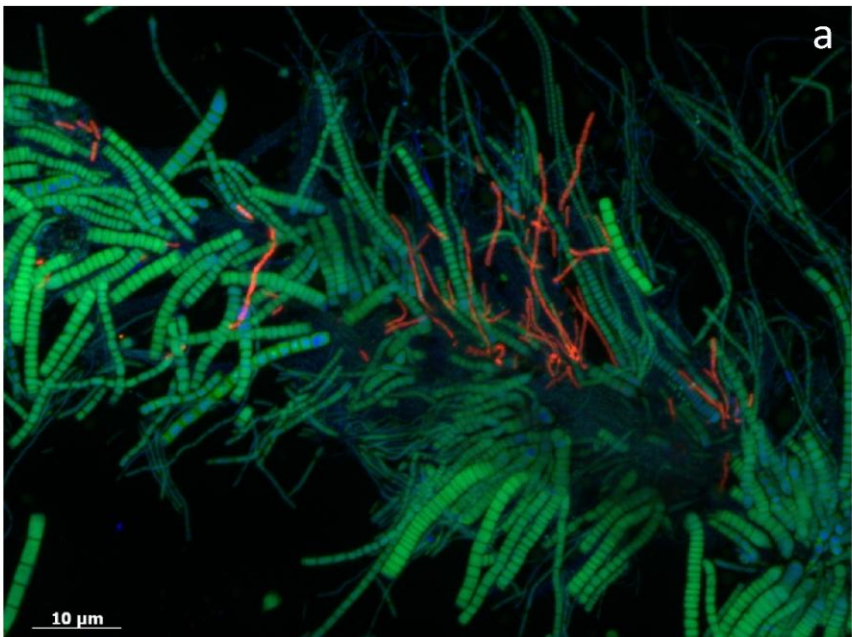
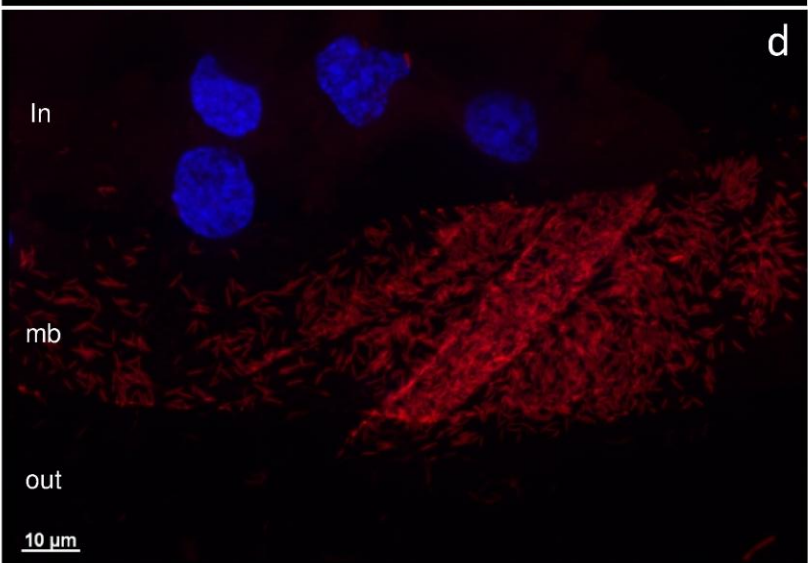
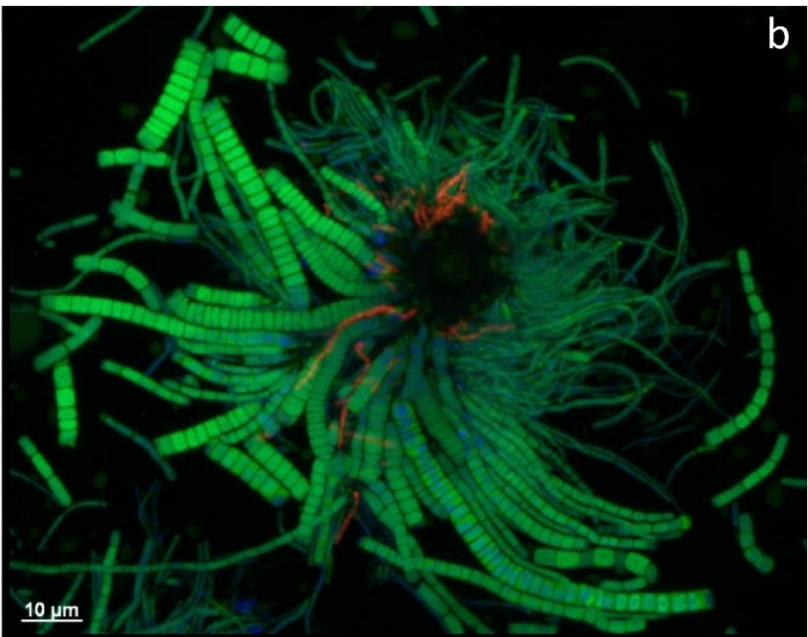
951

952

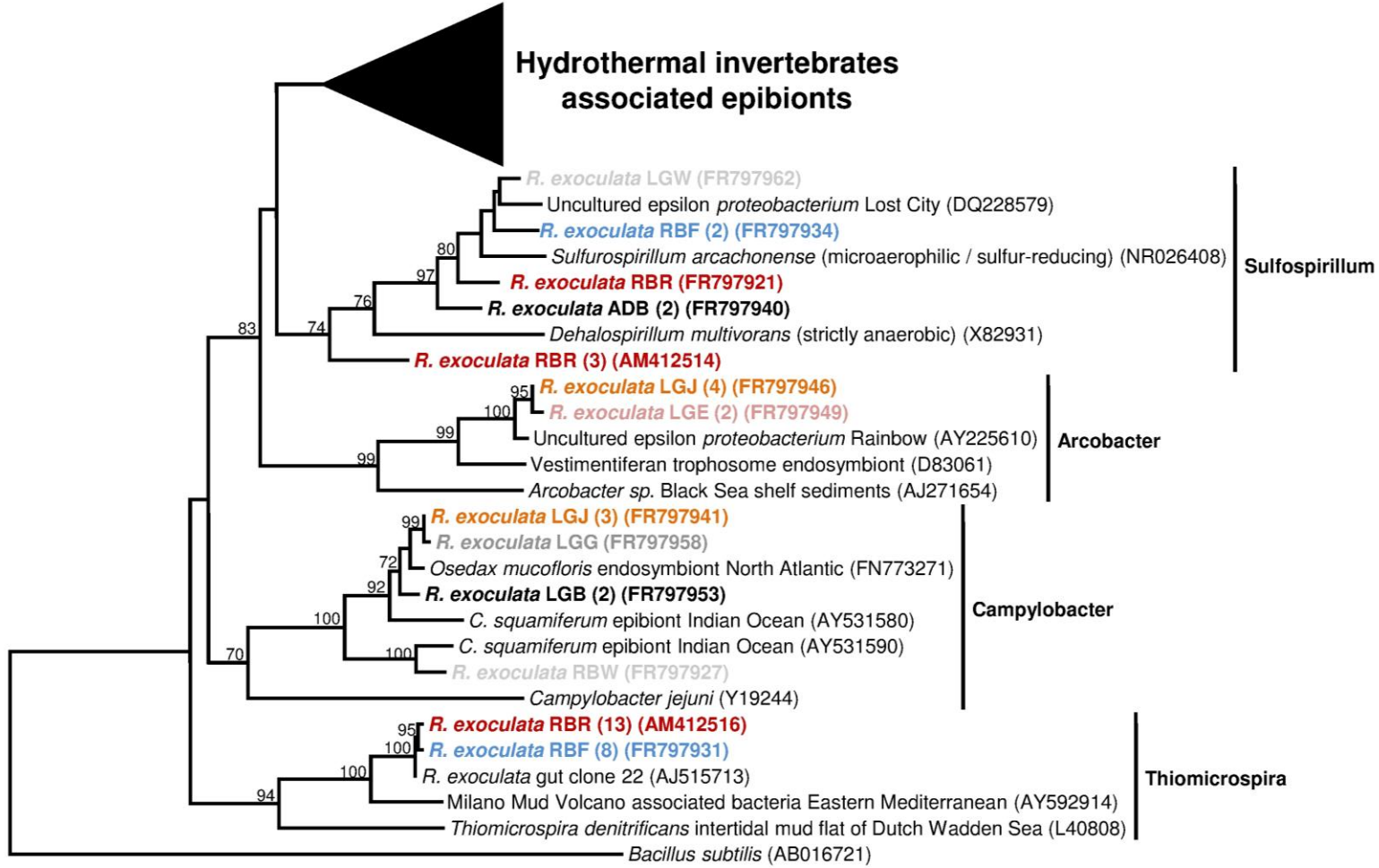
953

954

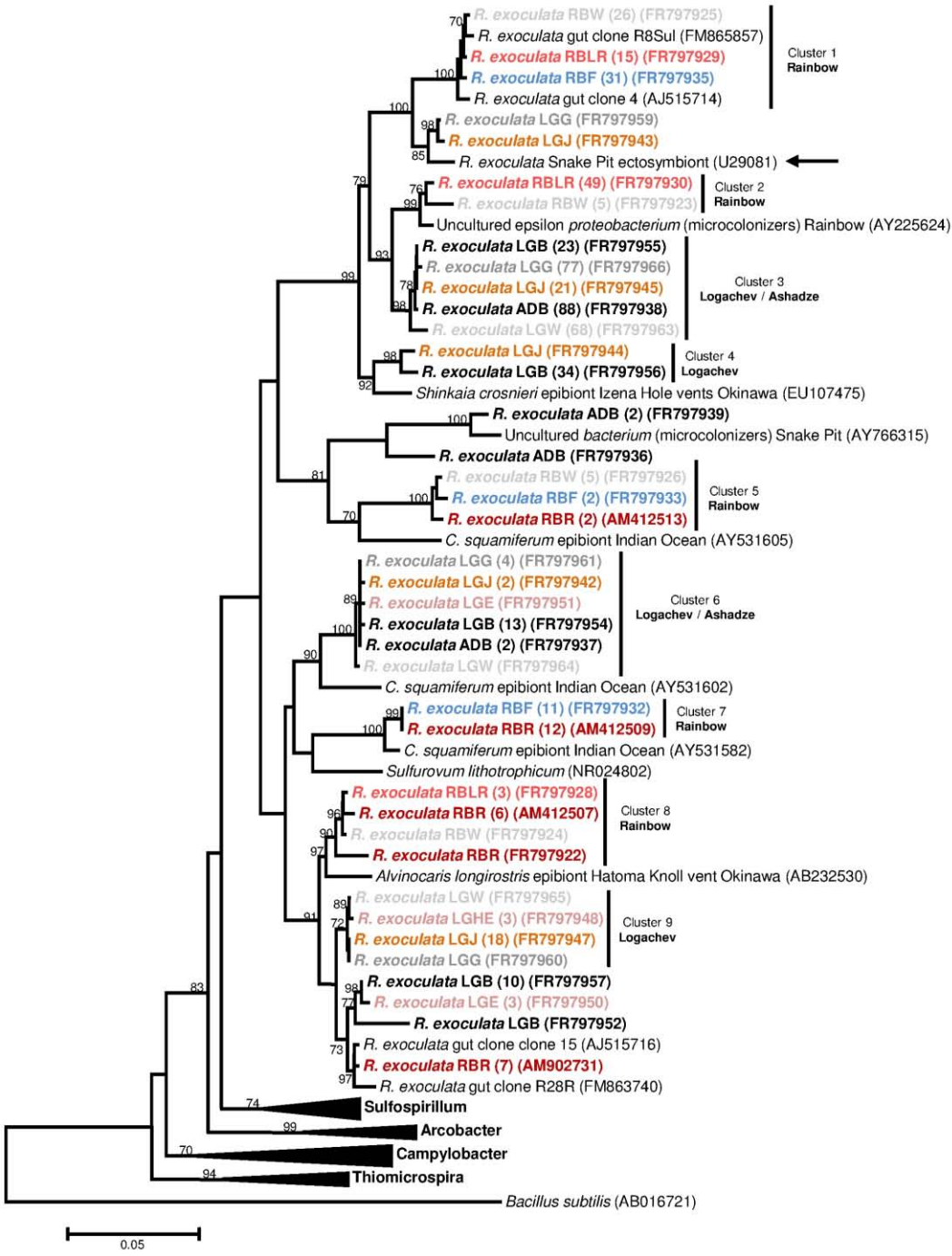
955



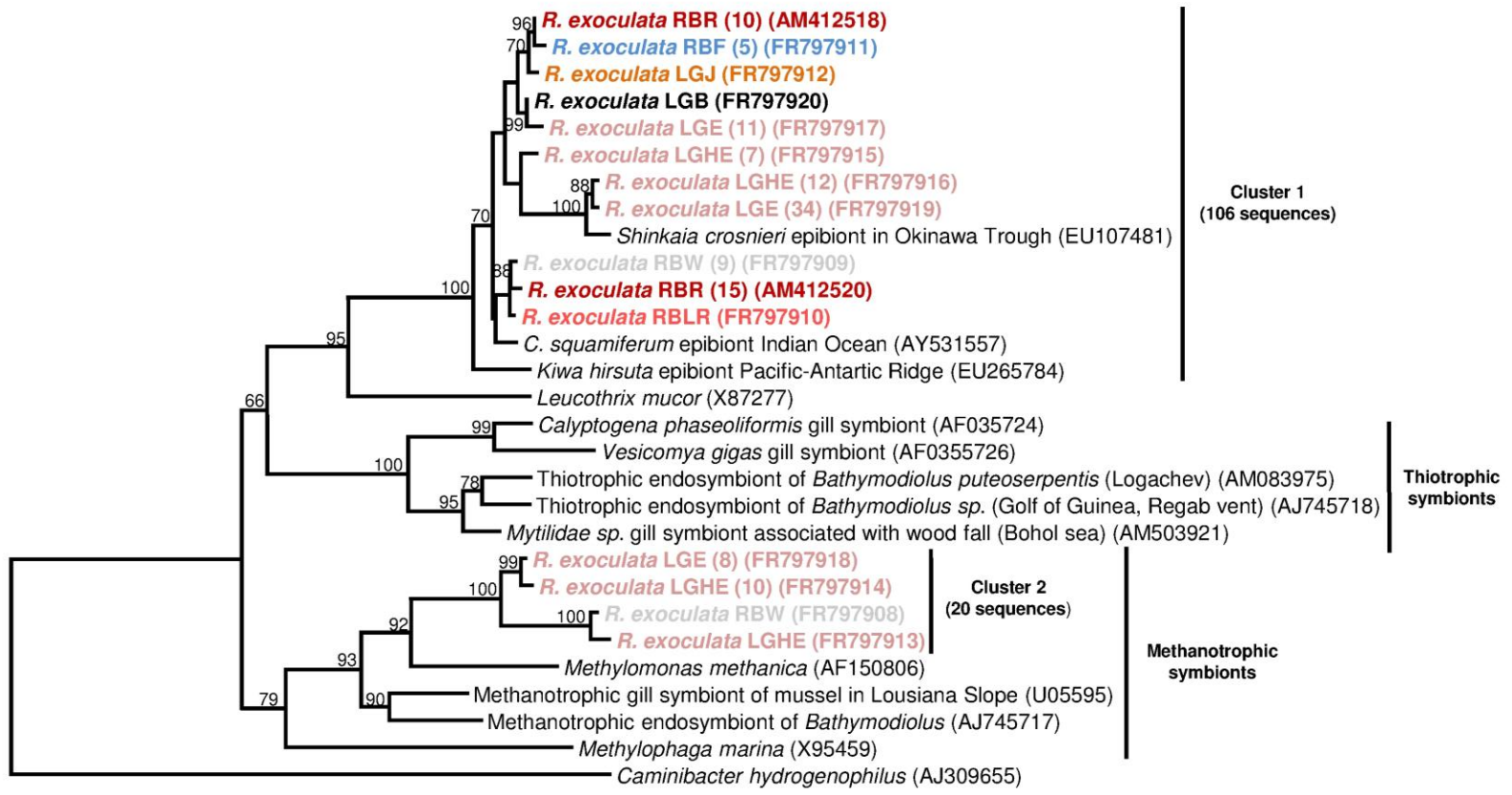
979
978
977
976
975
974
973
972
971
970
969
968
967
966
965
964
963
962
961
960
959
958
957
956



980
981
982
983
984
985
986
987
988
989
990
991
992
993
994
995
996
997
998
999
1000
1001
1002
1003



1004
1005
1006
1007
1008
1009
1010
1011
1012
1013
1014
1015
1016
1017
1018
1019
1020
1021
1022
1023
1024
1025
1026
1027



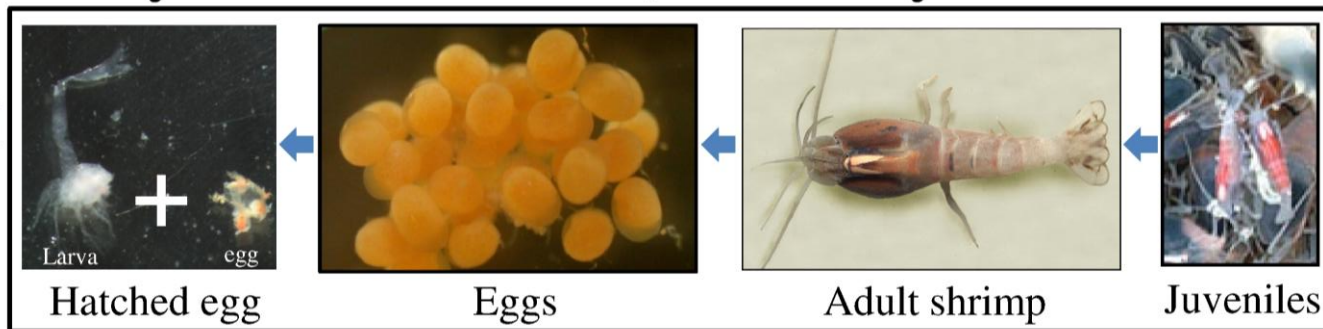
1028
1029
1030
1031
1032
1033
1034
1035
1036
1037
1038
1039
1040
1041
1042
1043
1044
1045
1046
1047
1048
1049
1050
1051

Water column, planktotrophic life ?

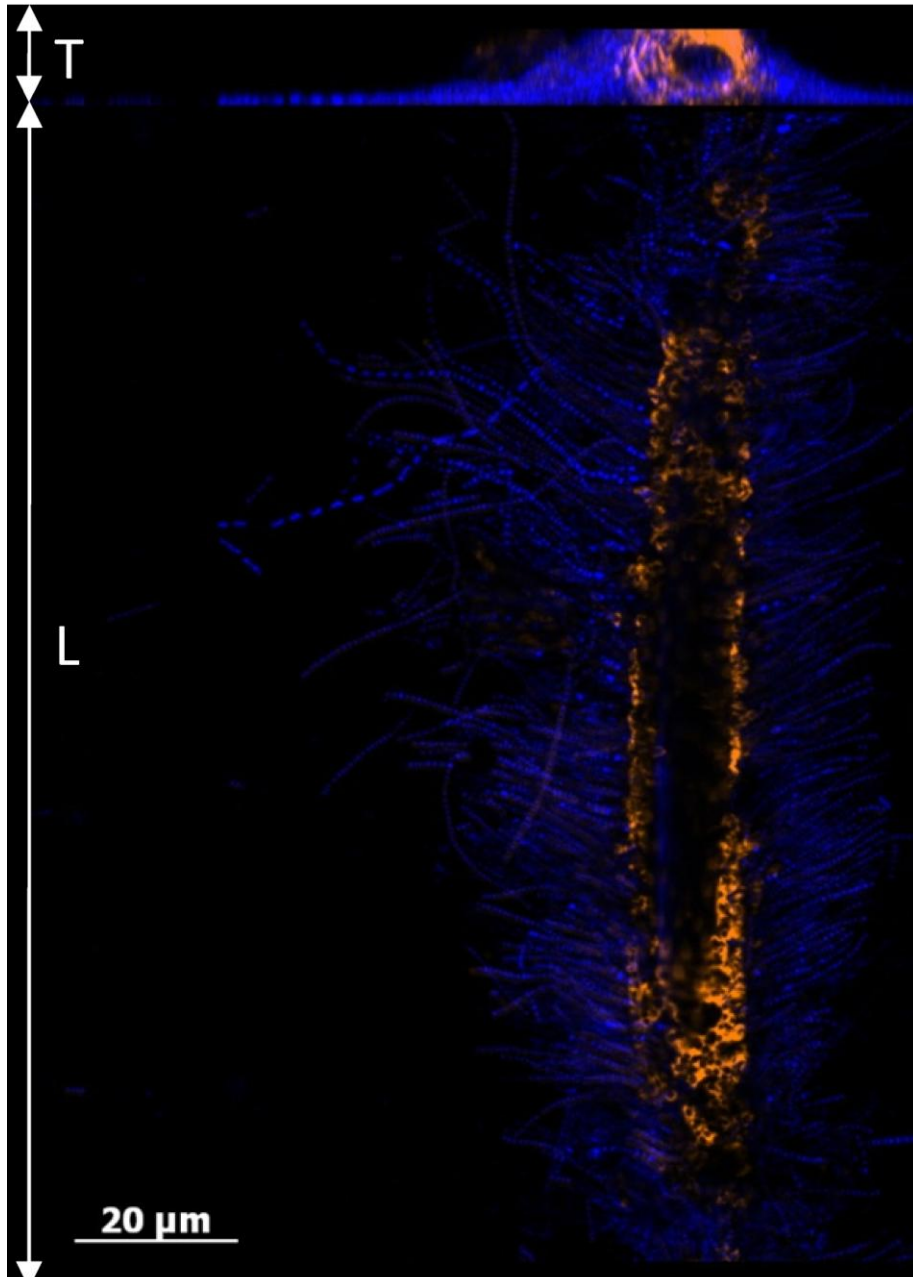
Dispersion ?

Recruitment ?

Hydrothermal vent, chimiosynthetic life

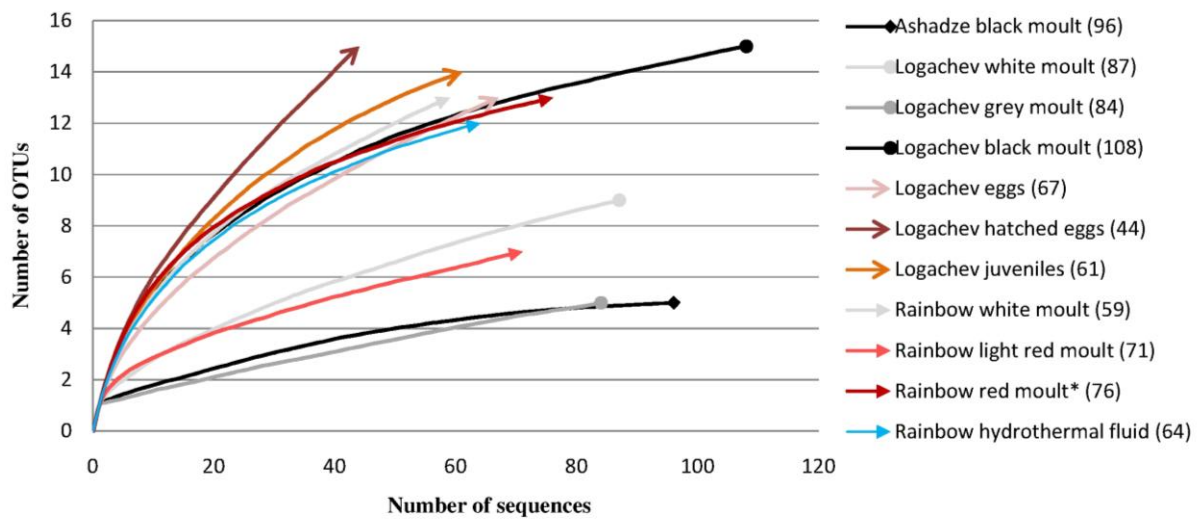


Supporting information



1069

1070 **Figure S1:** Longitudinal (L) and transversal (T) views of Scaphognathite setae
1071 from Rainbow shrimp with epibionts. The methanotrophic Gamma symbiont
1072 (orange) was hybridized with both LBI32/130 and GAM42a probes. The DAPI
1073 stained are in blue.



1074

1075

1076 **Figure S2:** Rarefaction curves (*by Zbinden *et al.* 2008).

1077

1078

1079

1080

1081

1082

1083

1084



1085 **Figure S3:** Picture showing the presence of *R. exoculata* orange juvenile nursery

1086 (on the bottom right hand corner) in shrimp aggregates.

1087 **Table S1:** Analysis of bacterial diversity associated with *R. exoculata* (gill
 1088 chamber and eggs). ¹Simpson indices values are presented as 1-H for best readability, the
 1089 diversity increasing from 0 (one species) to 1 (maximal diversity). ² by Zbinden *et al.* 2008.

	Library	Number of clones	OTUs number (97% similarity)	Good's coverage	1-H _{Simpson} ¹
1090	Ashadze black moult	96	5	98	0,16
	Logachev eggs	67	13	82	0,71
1091	Logachev hatched eggs	44	15	87	0,86
	Logachev juvenile	61	14	93	0,82
	Logachev white moult	87	9	92	0,38
1092	Logachev grey moult	84	5	97	0,12
	Logachev black moult	108	15	92	0,80
	Rainbow white moult	59	13	92	0,77
1093	Rainbow light red moult	71	7	95	0,48
	Rainbow red moult ²	76	13	97	0,84
1094	Rainbow hydrothermal fluid	64	12	95	0,77

1095

1096 **Table S2:** List of specimens and treatment.

1097 * Zbinden *et al.*, 2008.

1098 ¹Values for Rainbow are from Charlou *et al.*, 2002, for Logachev from Schmidt *et al.*, 2007, and for
 1099 Ashadze from Charlou *et al.*, 2010.

1100 This table shows the number of shrimps used by analyses.

	Pure fluid chemistry ¹					Number of sample per Analyzed					
	Ultramafic Hydrothermal site	Depth (m)	H ₂ S (mM)	H ₂ (mM)	CH ₄ (mM)	Stage / Sampling	16SrRNA	FISH	SEM	TEM	Total
1102						<i>R. exoculata</i> orange juvenile (2 cm, stage A)	-	2	-	-	2
						<i>R. exoculata</i> adult white moult	2	3	2	-	7
1103	Rainbow (36°13'N; 33°54'W)	2350	1.2	16	2.5	<i>R. exoculata</i> adult light red moult	2	3	2	-	7
						<i>R. exoculata</i> adult red moult	2*	3	2	1	9
						Hydrothermal fluid inside shrimp aggregates	+	-	-	-	-
1104						<i>R. exoculata</i> gravid female (number of eggs treated)	1(20+20) + 1(20+20)	1 (20)	1 (20)	1 (20)	4 (120)
						<i>R. exoculata</i> gravid female with hatched eggs + larvae (number of hatched eggs + larvae)	1(20+20+20)				1 (60)
						<i>R. exoculata</i> orange juvenile (2 cm, stage A)	2	3	2	-	7
1105	Logachev (14°45'N; 44°57'W)	3037	2.5	19	3.5	<i>R. exoculata</i> adult white moult	2	3	2	-	7
						<i>R. exoculata</i> adult grey moult	2	3	2	-	7
						<i>R. exoculata</i> adult black moult	2	3	2	-	7
	Ashadze (12°58'N; 44°51'W)	4080	1	8/19	0,5/1,2	<i>R. exoculata</i> adult black moult	2	3	2	-	7

65

1106

1107

1108

1109

1110

1111

1112

1113 **Tables S3: Closest match of representative 16S rRNA gene clone sequences**1114 (*by Zbinden *et al.*, 2008).

1115

Phylogenetic group	Representative clone sequences	Hit of BLAST (accession no.)	Similarity (%)	
<i>Epsilonproteobacteria</i>	RBR (AM412516)*, RBF (FR797931)	<i>R. exoculata</i> gut clone 22 (AJ515713)	99	
	RBW (FR797927)	<i>C. squamiferum</i> epibiont Indian Ocean clone SFC23D7 (AY531590)	97	
	LGB (FR797953), LGG (FR797958), LGJ (FR797941)	<i>Osedax mucofloris</i> endosymbiont North Atlantic clone 0mu3c42 (FN773271)	97-99	
	LGJ (FR797946), LGE (FR797949)	<i>Epsilonproteobacteria</i> Rainbow clone ATpp13 (AY225610)	98	
	RBR (AM412514)*	Uncultured <i>bacterium</i> clone FS1402B02 (AY704396)	93	
	ADB (FR797940)	Uncultured <i>bacterium</i> clone SGYF448 (FJ792213)	96	
	RBR (FR797921)*	<i>Sulfospirillum carboxydovorans</i> strain MV (AY740528)	94	
	RBF (FR797934)	<i>Epsilon-proteobacterium</i> clone ATOS Iris 7 Rainbow 26 (AJ969489)	98	
	LGW (FR797962)	Uncultured <i>bacterium</i> clone SGYF450 (FJ792215)	96	
	RBW (FR797925)	Ectosymbiont of <i>R. exoculata</i> clone Rc20eps3 (FM203377)	99	
	RBLR (FR797929), RBF (FR797935)	Ectosymbiont of <i>R. exoculata</i> clone Rc18eps2 (FM203406)	99	
	LGG (FR797959), LGJ (FR797943)	<i>Epsilon-proteobacterium</i> clone aH8 (FN562827)	99	
	RBLR (FR797930)	<i>Epsilon-proteobacterium</i> Rainbow clone ATpp27 (AY225624)	99	
	RBW (FR797923)	Ectosymbiont of <i>R. exoculata</i> clone Rc18E7 (FM393026)	98	
	LGB (FR797955), LGG (FR797966), LGJ (FR797945), ADB (FR797938)	Ectosymbiont of <i>R. exoculata</i> clone LOG283/74FI (FM203395)	99	
	LGW (FR797963)	Ectosymbiont of <i>R. exoculata</i> clone LOG272/69P2C1 (FM203396)	99	
	LGJ (FR797944), LGB (FR797956)	<i>Epsilon-proteobacterium</i> clone aE8 (FN562833)	98	
	ADB (FR797936), ADB (FR797939)	Uncultured <i>bacterium</i> (microcolonizers) Snake Pit clone 3 (AY766315)	92-97	
	RBW (FR797926), RBF (FR797933)	<i>R. exoculata</i> gill clone SCaII15 (AM412513)	98-99	
	RBR (AM412513)*	<i>C. squamiferum</i> epibiont Indian Ocean clone SFC23F5 (AY531605)	92	
	LGG (FR797961), LGJ (FR797942), LGE (FR797951), LGB (FR797954), ADB (FR797937), LGW (FR797964)	<i>Venttiella sulfuris</i> associated bacteria clone e34 (FN429840)	99	
	RBF (FR797932)	<i>R. exoculata</i> gill clone LBI7 (AM412509)	98	
	LBI7 (AM412509)*	<i>C. squamiferum</i> epibiont Indian Ocean clone SFC23F4 (AY531582)	96	
	RBLR (FR797928), RBW (FR797924)	<i>R. exoculata</i> gill clone LBI16 (AM412507)	97-98	
	RBR (AM412507)*	<i>Epsilon-proteobacterium</i> clone bC9 (FN562855)	96	
	RBR (FR797922)	Uncultured <i>bacterium</i> clone 102B111 (EF687148)	94	
	LGW (FR797965), LGHE (FR797948), LGJ (FR797947), LGG (FR797960)	<i>R. exoculata</i> gut clone R28R (FM863740)	98	
	LGB (FR797957), LGE (FR797950), LGB (FR797952)	<i>Epsilon-proteobacterium</i> clone bH8 (FN562857)	96-100	
	RBR (AM902731)*	<i>R. exoculata</i> gut clone 15 (AJ515716)	99	
	<i>Gammaproteobacteria</i>	RBR (AM412518)*	Ectosymbiont of <i>R. exoculata</i> clone Rc20gam1 (FM203378)	98
		RBF (FR797911), LGJ (FR797912)	<i>R. exoculata</i> gill clone LBI32 (AM412518)	99
		LGB (FR797920), LGE (FR797917)	Ectosymbiont of <i>R. exoculata</i> clone LOG272/69D1 (FN393024)	99
		LGHE (FR797915)	<i>R. exoculata</i> gill clone LBI32 (AM412518)	98
LGHE (FR797916), LGE (FR797919)		Uncultured <i>bacterium</i> clone Ba9 (FJ640825)	99	
RBW (FR797909), RBLR (FR797910)		<i>R. exoculata</i> gill clone SCaII16 (AM412520)	99	
RBR (AM412520)*		Ectosymbiont of <i>R. exoculata</i> clone Rc16gam3 (FM203375)	97	
LGE (FR797918), LGHE (FR797914)		<i>Gamma-proteobacterium</i> (methane oxidizer) clone HMMV Cen4 (AJ704661)	99	
RBW (FR797908), LGHE (FR797913)		<i>Gamma-proteobacterium</i> clone IBNC12 (AB175550)	98	